Bulletin of the *Transilvania* University of Brasov
Series II: Forestry • Wood Industry • Agricultural Food Engineering • Vol. 18(67) No. 3 – 2025
https://doi.org/10.31926/but.fwiafe.2025.18.67.3.6

MECHANICAL, PHYSICAL, AND SOUND ABSORPTION PROPERTIES OF WOOD-BASED COMPOSITES MADE FROM KRAJOOD (*Lepironia articulata)* USING ISOCYANATE AS BINDER

Chainarong SRIVABUT[1] Pruttipong PANTAMANATSOPA[1]
Chatree HOMKHIEW[2] Worapong BOONCHOUYTAN[2]
Surasit RAWANGWONG[2]

Abstract: *This study investigates the mechanical, physical, acoustic, and morphological properties of composites prepared from Krajood (Lepironia articulata) fibers bonded with isocyanate binder. The wood-based were fabricated with different fiber lengths (10 mm, 20 mm, and mixed lengths) and varied fiber-to-binder ratios of 80:20, 85:15, and 90:10 wt% using a compression molding process. The results showed that tensile strength and surface hardness significantly improved in composites with mixed fiber lengths, especially at an optimized fiber-to-binder ratio of 85:15 wt%. Additionally, water absorption and thickness swelling tests showed that higher binder content and shorter fibers effectively reduced moisture uptake, enhancing dimensional stability. Composites containing mixed fiber lengths showed the lowest water uptake and swelling values due to improved fiber packing density. Sound absorption analysis revealed superior acoustic performance at mid-range frequencies (500–2000 Hz) for composites with 20 mm fibers and mixed fibers, attributed to increased internal porosity and fiber scattering. Optical microscopy analysis demonstrated that composites with mixed fiber lengths displayed the most uniform and compact surface structures, with minimal fiber pull-out and porosity, suggesting enhanced fiber dispersion and matrix encapsulation. These findings highlight the critical role of fiber length distribution and binder ratio in tailoring composite properties. The optimized Krajood composites demonstrated a favorable balance between mechanical integrity, dimensional stability, and acoustic efficiency, highlighting their potential for sustainable applications such as eco-friendly interior components, elderly-supportive furniture, and acoustic panels.*

[1] Department of Industrial Engineering, Faculty of Engineering, Rajamangala University of Technology Srivijaya, Muang District, Songkhla 90000, Thailand;
[2] Materials Processing Technology Research Unit, Department of Industrial Engineering, Faculty of Engineering, Rajamangala University of Techn, ology Srivijaya, Muang District, Songkhla 90000, Thailand;
Correspondence: Chainarong Srivabut; email: chainarong.s@rmutsv.ac.th.

Key words: *wood-based composites, isocyanate glue, Krajood fiber, mechanical properties, sound absorption.*

1. Introduction

The growing demand for environmentally sustainable and high-performance materials is intensified research interest in natural fiber-reinforced polymer composites [1, 2]. These bio-composites, comprising plant-based fibers embedded in polymeric matrices, present promising alternatives to conventional synthetic composites due to their biodegradability, low density, renewability, and favorable mechanical properties [11, 26]. Among the various natural fibers available, lignocellulosic fibers such as jute, flax, kenaf, and, more recently, Krajood (*Lepironia articulata*), have attracted considerable attention for engineering applications. Particularly abundant in Southeast Asia, and especially Thailand, Krajood fiber is characterized by its high cellulose content, low cost, and local availability, making it an attractive candidate for composite reinforcement [14]. However, the inherent mechanical and dimensional limitations of raw natural fibers necessitate optimization in terms of processing techniques, fiber treatments, and fiber-matrix compatibility to maximize their performance [6, 19].

Despite the inherent advantages of natural fiber composites, several challenges remain in tailoring their performance for structural and semi-structural applications. Variability in fiber morphology, inconsistent fiber contents, and weak interfacial bonding between hydrophilic fibers and hydrophobic polymeric matrices often result in reduced mechanical strength and dimensional instability [2, 15, 30]. Furthermore, limited moisture resistance and inferior acoustic insulation properties compared to synthetic composites hinder broader adoption [21, 29]. The integration of suitable thermosetting binders, such as isocyanate resins, presents a promising solution for enhancing fiber and matrix adhesion and overall composite integrity. However, the relationship between fiber size distribution, fiber content, and binder proportion in determining the final performance characteristics of wood-based composites remains insufficiently understood [21, 22].

While previous studies have explored various natural fiber composites, a notable gap persists in systematically evaluating the combined effects of fiber length distributions and fiber-to-binder mixing ratios on composite properties using compression molding techniques [1, 23]. Most existing research tends to focus on single-fiber-size systems or general mechanical testing, while comprehensive analyses involving simultaneous assessment of mechanical properties (tensile and hardness), physical (moisture resistance), and functional performance (sound absorption properties) under varying fabrication parameters are limited [17, 20]. Additionally, detailed experimental evidence elucidating how mixed fiber lengths influence stress distribution, acoustic behavior, and dimensional stability in composites bonded with isocyanate-based systems is scarce [11, 12, 27].

To address these gaps, this study investigates the fabrication and

comprehensive characterization of wood-based composites reinforced with Krajood fibers and bonded using isocyanate binder via compression molding [14]. Specifically, the study explores the effects of fiber lengths (10 mm, 20 mm, and mixed sizes) and fiber-to-binder ratios on the mechanical, physical, sound absorption, and morphological properties of these composites. Mechanical properties, including tensile strength and modulus of the samples, are systematically assessed [7, 29]. Dimensional stability is evaluated through water absorption test, while acoustic performance is measured by sound absorption coefficients across various frequency ranges. Optical microscopy is employed to examine the composite surface morphology, providing additional insights into fiber dispersion and fiber matrix interactions [28, 31].

The contributions of this research are threefold. First, it establishes clear empirical relationships between fiber morphology, binder content, and resulting composite performance, providing valuable quantitative data to inform composite design. Second, it introduces a hybrid approach by combining short and long fibers to optimize the internal structure, thereby enhancing both mechanical integrity and acoustic attenuation capacity [8, 24]. Third, the study demonstrates the effectiveness and scalability of using isocyanate binders within a compression molding framework for natural fiber composites. Collectively, these findings contribute to the advancement of sustainable material development, facilitating broader utilization of natural fiber-reinforced composites in construction, furniture manufacturing, and acoustic insulation applications [9, 10].

Consequently, the primary objectives of this research include identifying optimal mixture ratios of Krajood fibers and isocyanate binder to achieve superior mechanical, physical, and acoustic properties, as well as providing a foundation for future developments in intelligent and sustainable manufacturing practices within the bio-composite industry.

2. Materials and Methods

2.1. Materials

The Krajood (*Lepironia articulata*) fibers used in this study were sourced from local manufacturers producing handcraft from their waste materials. Prior to composites fabrication, the Krajood fibers were sieved into two distinct size classes: short (10 mm) and long (20 mm). Subsequently, the fibers were dried in an oven at 110°C for 8 hours to ensure the moisture content was reduced below 1%. Isocyanate binder (UP-H960), characterized by a heat resistance capability up to 250°C, was acquired from Three Bond VIV Sales Co., Ltd. (Bangkok, Thailand).

2.2. Preparation of Composite Panels and Specimens

The composite panels were fabricated in three primary steps. Initially, Krajood fibers and isocyanate binder were weighed according to the designed fiber-to-binder ratios (Table 1) and thoroughly mixed at room temperature for 5 min to achieve homogeneity. Next, the fiber-binder mixture was processed using a compression molding (hot-press) machine at a temperature of 180°C and a pressure of 2000 psi for 25 min [14]. This molding process involved sequential phases: pre-

heating (5 min), pressing (10 min), and cooling with water (10 min). Finally, the composite panels were machined into specimens according to American Society for Testing and Materials (ASTM) standards [14, 21, 26] prior to mechanical, physical, and acoustic evaluations.

Formulation of experimental composite panels Table 1

Formulations	Fiber size [mm]	Krajood fiber [wt%]	Isocyanate glue [wt%]
S80I20	10 (Short size; S)	80	20
S85I15		85	15
S90I10		90	10
L80I20	20 (Long size; L)	80	20
L85I15		85	15
L90I10		90	10
M80I20	10 and 20 (Mixed size; M)	80	20
M85I15		85	15
M90I10		90	10

Note: Short size (S), Long size (L), Mixed size (M), and Isocyanate glue (I).

2.3. Characterizations

2.3.1. Tensile Test of the Samples

The tensile properties were measured using an Instron Universal Testing Machine (Model 5582, Instron Corporation, MA, USA) following ASTM D638-91 standard [5]. Specimens (five replicates per formulation) were machined into dumbbell shapes from composite panels. All specimens were oven-dried at 50°C for 24 hours and tested at a crosshead speed of 5 mm/min.

2.3.2. Hardness Test of the Samples

Shore D hardness values were determined according to ASTM D2240-91 [3] using a Shore D Durometer (Model GS-702G, Teclock Corporation, Nagano, Japan). Five replicates per formulation (dimensions: 30 mm × 30 mm × 6 mm) were oven-dried at 50°C for 24 hours prior to testing. All measurements were conducted at room temperature (25°C).

2.3.3. Water Absorption and Thickness Swelling Test of the Samples

Short-term water absorption (*WA*) and thickness swelling (*TS*) were evaluated according to ASTM D570-88 specifications [4]. Composite specimens (10 mm × 20 mm × 6 mm, five replicates per formulation) were immersed in distilled water at room temperature (25°C) for durations of 2 and 24 hours. Before immersion, all specimens were dried at 50°C for 24 hours. Following immersion, specimens were removed, gently wiped with tissue paper, and immediately weighed and measured to calculate *WA* and *TS* percentages as follows in Equations (1) and (2).

$$WA_t = \frac{M_2 - M_1}{M_1} \cdot 100 \quad (1)$$

where:

WA_t is the water absorption at time t [%];
M_1 and M_2 – the specimen weight before and after immersion, respectively [g].

$$TS_t = \frac{T_2 - T_1}{T_1} \cdot 100 \quad (2)$$

where:

TS_t is the thickness swelling at time t [%];

T_1 and T_2 – the specimen thickness before and after immersion, respectively [mm].

2.3.4. Sound Absorption Test of the Samples

The sound absorption properties were measured following ISO 10534 standard [16] using an impedance tube (Acoustic Material Testing Type 3560 B-T72/X72, Bruel & Kjaer, Naerum, Denmark) with a tube diameter of 30 mm. Composite specimens were evaluated at frequencies of 250, 500, 1000, and 2000 Hz to determine sound absorption coefficients and Noise Reduction Coefficient (*NRC*). Specimens were placed at one end of the tube opposite to a speaker emitting white noise. Measurements were repeated for five replicates per formulation at room temperature (25°C). The experimental setup is illustrated in Figure 1.

2.3.5. Optical Microscopy Analysis

Surface morphology was examined using optical microscopy (Axioskop 5 MAT, Zeiss, Oberkochen, Germany) at a magnification of 100×. The specimens were oven-dried at 50°C for 24 hours prior to examination.

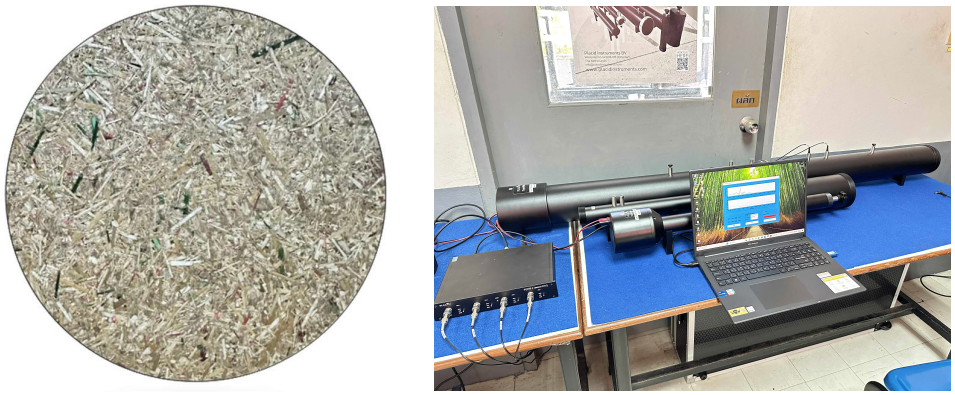

a. b.

Fig. 1. *Specimens and sound absorption test process*

2.4. Statistical analysis

A one-way analysis of variance (ANOVA) was conducted to statistically evaluate the significance of the effects of the fiber lengths and fiber-to-binder ratios on the composite properties (tensile strength, hardness, *WA*, *TS*, and acoustic performance – Table 2). All statistical analyses were performed at a significant level of $\alpha = 0.05$.

Mechanical and physical properties of Krajood composites Table 2

Formulations [wt%]	Fiber sizes [mm]	Tensile		Hardness	Water	Thickness
		Strength [MPa]	Modulus [GPa]	(Shore D)	Absorption [%]	Swelling [%]
S80I20	10	22.04	0.67	71.45	10.23	8.12
S85I15		20.59	0.86	68.32	12.34	10.67
S90I10		18.44	0.90	63.45	16.56	14.90
P-value	**-**	***0.000****	***0.001****	***0.000****	***0.000***	***0.001****
L80I20	20	30.56	0.83	74.34	20.44	17.44
L85I15		26.45	0.94	72.56	23.55	19.55
L90I10		23.07	0.98	70.89	25.56	22.78
P-value	**-**	***0.000****	***0.001****	***0.000****	***0.000****	***0.001****
M80I20	10 and 20	33.43	0.95	78.56	13.21	10.66
M85I15		31.89	1.02	75.34	15.66	14.61
M90I10		25.27	1.23	72.12	18.34	16.91
P-value	**-**	***0.000****	***0.001****	***0.000***	***0.000***	***0.001****

Note: Short size (S), Long size (L), Mixed size (M).

3. Results and Discussion

3.1. Tensile Properties of the Composites

Tensile strength and modulus are critical indicators of mechanical performance, particularly for applications subjected to tensile loads. The results presented in Table 2 reveal statistically significant differences across formulations ($p < 0.05$), highlighting the correlation between fiber size, fiber-to-binder ratio, and mechanical properties.

As shown in Figures 2a and 2b, short fiber composites (10 mm; S-series) exhibited reduced tensile strength with increasing fiber content (i.e., decreasing binder content), declining from 22.04 MPa (S80I20) to 18.44 MPa (S90I10). Conversely, tensile modulus increased from 0.67 GPa to 0.90 GPa as fiber content rose. This inverse trend highlights the trade-off between ductility and stiffness; higher fiber loadings enhance stiffness but may impair stress transfer efficiency if fiber wetting and fiber-matrix bonding become inadequate due to insufficient binder content. Consequently, despite increased stiffness, short fibers provide limited tensile strength owing to their lower aspect ratio and smaller interfacial bonding area [19, 26].

Long fiber composites (20 mm; L-series) outperformed short fiber composites in both tensile strength and modulus. Specifically, the L80I20 formulation reached a peak tensile strength of 30.56 MPa, approximately 39% higher than the equivalent short fiber formulation (S80I20). Additionally, tensile modulus increased with higher fiber content, peaking at 0.98 GPa for L90I10. This enhanced mechanical performance results from the higher aspect ratio of long fibers, which facilitates efficient stress bridging, improved fiber-matrix adhesion, and effective load transfer. Although a modest decrease in tensile strength occurred with reduced binder content (L80I20 to L90I10), this reduction was less significant compared to short fiber composites, highlighting the capability of long fibers to sustain mechanical properties under reduced binder availability, albeit with some compromise due to incomplete fiber

encapsulation [15, 21].

Mixed fiber composites (10 and 20 mm; M-series) displayed the highest overall mechanical performance among all tested formulations. The M80I20 composite recorded the maximum tensile strength (33.43 MPa), while the M90I10 composite exhibited the highest modulus (1.23 GPa). This significant improvement arises from the synergistic interaction between the different fiber sizes: longer fibers enhance stress transfer and energy dissipation, whereas shorter fibers fill gaps, reduce voids, and improve packing density, thus contributing to better matrix continuity and fiber dispersion. Mixed fiber composites, therefore, provide an optimal balance of load-bearing capacity and stiffness.

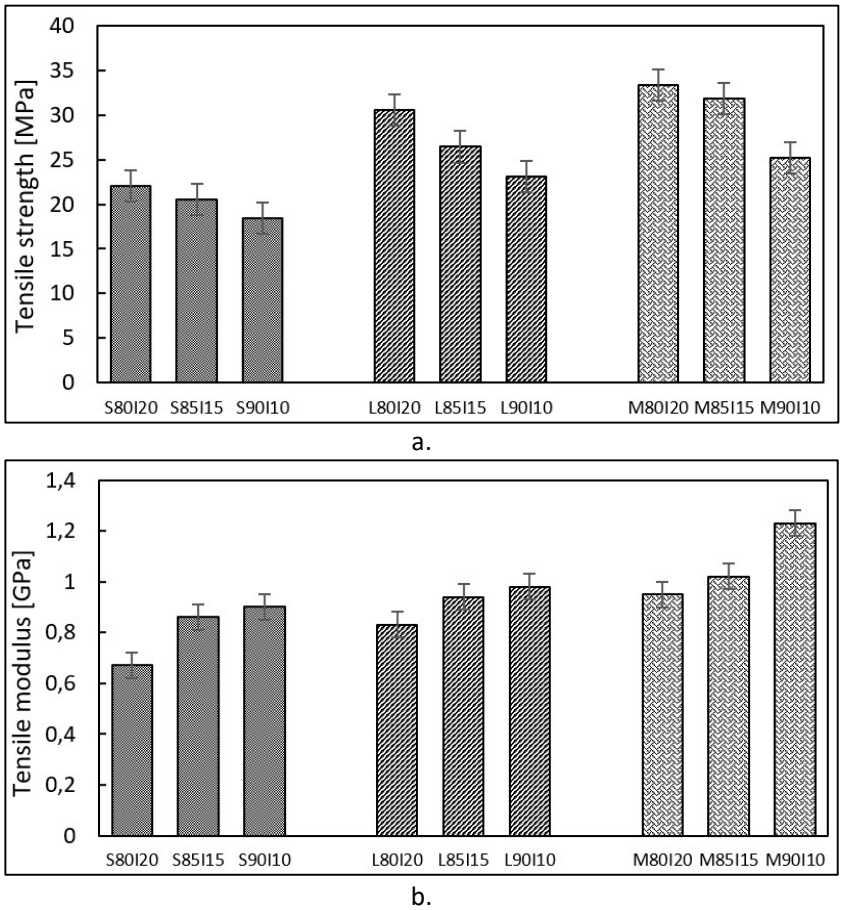

Fig. 2. *Tensile properties of Krajood composites with different fiber sizes and contents: a. tensile strength, and b. tensile modulus*

Analysis of variance (ANOVA) confirmed significant differences in tensile strength and modulus across all formulations ($p < 0.001$), affirming the measurable influence of fiber length and binder ratio on composite mechanical properties. Tensile

strength decreases at higher fiber contents due to insufficient binder coverage, while modulus consistently increases owing to the greater stiffness contribution from fibers. Mixed fiber systems outperform single fiber-size configurations by leveraging both macro- and micro-scale reinforcement effects. These findings emphasize the critical role of optimal binder content for achieving high tensile strength, especially in short fiber composites, and highlight the advantages of fiber hybridization in delivering composites that combine mechanical durability and structural stability [14, 31]. Consequently, the formulations M80I20 and M85I15 are recommended for high-performance, sustainable composite applications such as furniture components, wall panels, and load-bearing interior elements.

3.2. Hardness Properties of the Composites

Hardness is a mechanical parameter that reflects a material resistance to localized surface deformation, playing a vital role in determining the wear resistance and durability of composites, particularly in load bearing or impact-prone applications [11, 22]. In this study, Shore D hardness was used to evaluate the surface integrity of wood-based composites reinforced with Krajood fibers of varying lengths (S-series, L-series, and M-series) and different fiber-to-binder ratios. The results, summarized in Table 2, demonstrate that both fiber morphology and binder content significantly affect composite hardness (p-value = 0.000).

The S-series composites showed a declining trend in hardness as binder content decreased. Shore D hardness dropped from 71.45 (S80I20) to 68.32 (S85I15), and further to 63.45 (S90I10). This reduction highlights the critical role of isocyanate binder in forming a rigid matrix capable of resisting surface indentation. Lower binder content likely results in a more porous and less cohesive matrix, reducing its capacity to maintain surface integrity. Additionally, short fibers provide limited load distribution efficiency due to their lower aspect ratio, further compromising reinforcement and hardness.

In contrast, the L-series composites exhibited consistently higher hardness values than their S-series. Shore D hardness ranged from 74.34 (L80I20) to 70.89 (L90I10), with a more gradual decline observed as binder content decreased. The enhanced hardness performance is attributed to the improved stress transfer and fiber-matrix interlocking offered by longer fibers. Notably, even at the lowest binder ratio (L90I10), the hardness remained higher than that of the S80I20 sample, emphasizing the superior structural reinforcement provided by the L-series.

The M-series displayed the highest overall hardness among all formulations. M80I20 achieved the higest hardness value of 78.56 Shore D, followed by M85I15 (75.34) and M90I10 (72.12). This superior performance reflects a synergistic reinforcement mechanism wherein short fibers enhance packing density and fill microvoids, while long fibers contribute macro-scale stiffness and stress bridging. This multi-scale reinforcement approach results in improved composite compactness and surface resistance to deformation [17, 23].

All Shore D hardness test results for the various fiber sizes and contents are

illustrated in Figure 3. ANOVA confirmed statistically significant differences within each fiber group (p-value = 0.000). Comparing across groups, it is evident that hardness is positively influenced by both binder content and fiber architecture. The M-series consistently outperformed single-size fiber systems, likely due to better interfacial bonding and optimized fiber packing.

The M80I20 formulation exhibited a 10% increase in hardness compared to the best-performing L-series sample and approximately a 24% improvement over the lowest-performing S-series sample. These findings highlight the critical role of binder content in maintaining surface hardness, particularly in composites with S-series. The L-series enhance structural integrity, contributing to improved surface mechanical behavior. However, the M-series proves most effective, offering significant gains in hardness through multi-scale reinforcement.

Such enhancements are particularly valuable in applications requiring high wear resistance, dimensional stability, and mechanical durability, including floor panels, cabinetry, and impact-resistant furniture surfaces fabricated from bio-based composite materials [18, 19].

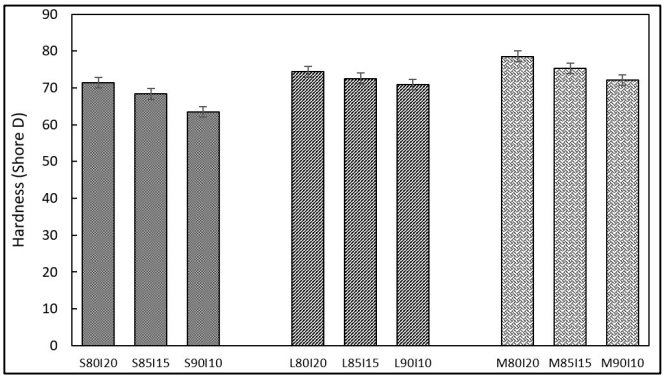

Fig. 3. *Hardness property of Krajood composites with different fiber sizes and contents*

3.3. Water Absorption and Thickness Swelling Properties of the Composites

Water absorption (*WA*) and thickness swelling (*TS*) are critical indicators of the dimensional stability and long-term durability of wood-based composites, particularly in moisture-rich environments [22, 23]. Table 2 summarizes the experimental results for *WA* and *TS* in composites reinforced with Krajood fibers of varying lengths and different fiber-to-isocyanate binder ratios. The findings indicate that both properties are significantly influenced by fiber size distribution and binder content, with all p-values < 0.05, confirming strong statistical significance. The effects of fiber size and binder content on *WA* and *TS* are illustrated in Figures 4a and 4b.

The S-series composites exhibited relatively low *WA* and *TS*, especially at higher binder contents. The S80I20 formulation showed the lowest *WA* at 10.23% and *TS* at 8.12%. However, as binder content decreased, both *WA* and *TS* increased substantially, reaching 16.56 and 14.90%, respectively, for the S90I10

formulation. This trend highlights the critical role of binder in forming a dense, hydrophobic matrix that limits moisture penetration. Short fibers, with their lower aspect ratio and reduced porosity pathways, inherently resist water uptake more effectively. However, when binder content is insufficient, poor fiber encapsulation leads to increased hygroscopic response.

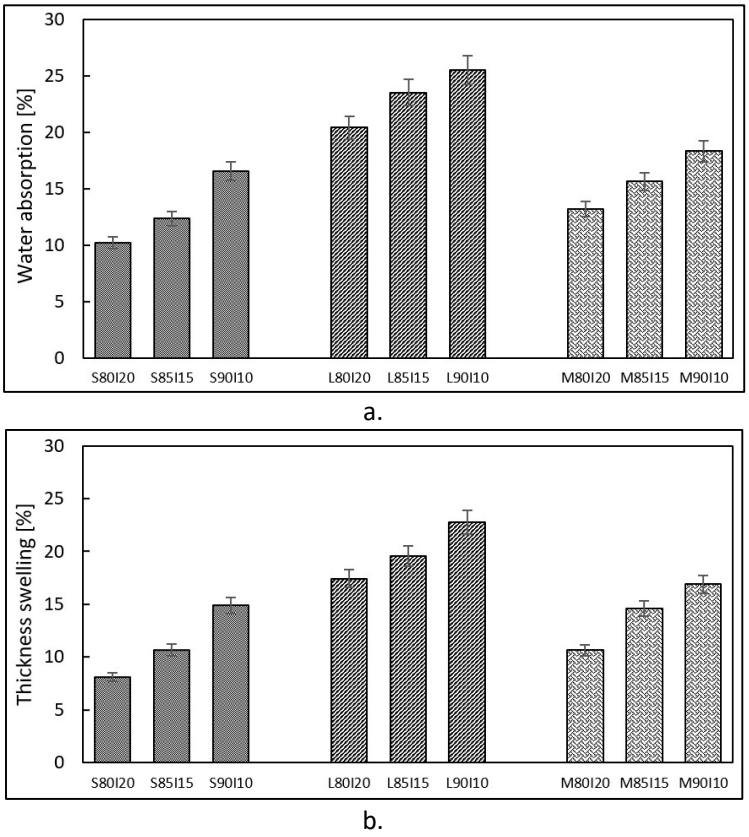

Fig. 4. *Water absorption (a.) and thickness (b.) swelling properties of Krajood composites with different fiber sizes and contents*

The L-series composites, by contrast, demonstrated significantly higher *WA* and *TS* values. The L80I20 formulation recorded a *WA* of 20.44% and a *TS* of 17.44%, which further increased to 25.56 and 2.78%, respectively, in the L90I10 formulation. These elevated values are attributed to the greater capillarity and increased fiber-matrix interface exposure of long fibers, which create continuous channels for moisture ingress. Although long fibers contribute positively to mechanical strength, their hydrophilic nature and extensive surface area challenge dimensional stability particularly when binder content is too low to fully encapsulate the fibers.

The intermediate performance between the S- and L-series. The M80I20 sample achieved a *WA* of 13.21% and a *TS* of

10.66%, while M90I10 reached 18.34 and 16.91%, respectively. These results suggest that the M-series architecture optimize internal fiber packing and reduce the formation of capillary channels, effectively mitigating water ingress while maintaining mechanical benefits provided by the L-series. This balance supports fiber size hybridization as a promising strategy for enhancing moisture resistance without compromising structural integrity [15, 17].

ANOVA analysis further confirmed that both fiber type and binder ratio significantly affected *WA* and *TS* ($p < 0.05$). Among all formulations, the S-series, particularly S80I20, exhibited the best dimensional stability, underscoring the importance of sufficient binder and shorter fiber lengths in resisting water-related degradation. In contrast, the L-series showed the poorest performance, emphasizing the need for additional surface treatments or improved matrix encapsulation for long fiber composites. The M-series composites served as an effective compromise, balancing structural performance with moisture resistance.

These results lead to several key insights. Higher isocyanate content significantly reduces *WA* and *TS* by improving matrix cohesion and minimizing porosity. Shorter fibers limit moisturizing transport pathways, enhancing stability but potentially limiting strength [12, 25]. The M-series provide multifunctional advantages, allowing composite designers to tailor materials for both mechanical and environmental performance. Given their balance between mechanical robustness and dimensional stability, the M80I20 and S80I20 formulations are recommended for moisture-sensitive applications such as interior furniture panels, composite decking, and kitchen cabinetry made from sustainable lignocellulosic materials.

3.4. Sound Absorption Properties of the Composites

Sound absorption performance is a vital parameter for assessing the acoustic suitability of wood-based composites, particularly in indoor applications such as wall panels, acoustic boards, and sustainable interior furnishings [8, 28]. In this study, sound absorption coefficients were measured at frequencies of 250, 500, 1000, and 2000 Hz, and the Noise Reduction Coefficient (*NRC*) was determined as well as. The average of these four values was calculated to provide a comprehensive measure of acoustic performance. Table 3 summarizes the results for composites grouped by fiber size and resin formulation. ANOVA confirmed statistically significant differences across all test frequencies and *NRC* values ($p < 0.05$), validating the influence of fiber morphology and binder content on acoustic behavior.

The S-series demonstrated moderate sound absorption that improved with increasing fiber content. The S80I20 sample recorded an *NRC* of 0.32, with absorption coefficients ranging from 6.19% at 250 Hz to 11.20% at 2000 Hz. Enhanced fiber content in the S85I15 and S90I10 samples yielded *NRC* values of 0.38 and 0.56, respectively. This improvement is attributed to increased porosity and fiber–air interface surface area, which promote greater internal friction and sound wave scattering. However, the limited fiber length restricts wave penetration and energy dissipation, particularly at lower frequencies.

Sound absorption coefficient and NRC values of the Krajood composites Table 3

Code	Fiber sizes [mm]	Sound frequency [Hz]				Average [Hz]	NRC
		250	500	1000	2000		
S80I20	10 (Short size)	6.19	8.92	9.78	11.20	9.02	0.32
S85I15		6.80	9.81	12.67	14.50	10.95	0.38
S90I10		7.11	9.09	13.51	15.79	11.38	0.56
p-value	-	***0.001****	***0.002****	***0.000****	***0.002****	***0.001****	***0.001****
L80I20	20 (Long size)	6.29	8.78	11.44	13.62	10.03	0.33
L85I15		6.88	9.74	12.67	14.69	11.00	0.41
L90I10		8.11	10.67	14.12	15.81	12.18	0.65
p-value	-	***0.002****	***0.002****	***0.000****	***0.000****	***0.002****	***0.000****
M80I20	10 and 20 (Mixed size)	7.20	10.02	13.56	15.11	11.47	0.48
M85I15		7.89	11.74	13.99	16.70	12.58	0.68
M90I10		8.55	12.67	15.71	17.36	13.57	0.76
p-value	-	***0.001****	***0.001****	***0.000****	***0.000****	***0.000****	***0.000****

The L-series composites exhibited superior performance relative to the S-series, especially in the mid-to-high frequency range. The L90I10 formulation achieved the highest sound absorption in this group, recording 8.11% at 250 Hz, 14.12% at 1000 Hz, and 15.81% at 2000 Hz, with an *NRC* of 0.65. These improvements are attributed to the extended acoustic pathways enabled by longer fibers, which enhance wave attenuation and increase tortuosity of internal airflow, thereby amplifying viscous and thermal dissipation. However, excessive fiber length combined with insufficient binder (as in L90I10) may compromise structural cohesion, highlighting the need to balance acoustic performance with mechanical integrity.

The M-series composites demonstrated the highest overall acoustic absorption. The M90I10 formulation achieved an *NRC* of 0.76, the highest across all tested samples with absorption coefficients peaking at 8.55% (250 Hz) and 17.36% (2000 Hz). These results underscore the synergistic benefits of combining different fiber lengths. Short fibers enhance surface-level interaction, while long fibers contribute to deeper energy dissipation. The multiscale fiber architecture improves pore connectivity, airflow resistivity, and acoustic wave scattering, making these composites highly effective for sound-absorbing applications. Furthermore, the M85I15 sample, with slightly higher binder content, maintained a strong *NRC* of 0.68, offering a favorable balance between acoustic performance and mechanical stability.

ANOVA results across all frequency bands confirmed statistically significant differences ($p < 0.05$) both within and between fiber groups. All formulations benefited from increased fiber content, reflected in improved NRC values. While S90I10 and L90I10 demonstrated strong performance in their respective groups, neither matched the superior absorption capabilities of M90I10. These findings highlight the effectiveness of hybrid fiber architecture in optimizing sound absorption [14]. Higher fiber contents promote internal friction and energy dissipation, while long fibers enhance low- to mid-frequency performance and short fibers improve interaction with incident sound waves at the surface [29, 31].

Overall, the M-series presents an optimal

strategy for developing high-performance, sustainable acoustic panels with strong mechanical properties and excellent sound absorption. The M90I10 and M85I15 formulations are highly recommended for applications such as interior wall cladding, ceiling tiles, acoustic partitions, and other noise control systems where eco-friendly materials with high NRC values are desired.

3.5. Surface Observation of the Composites

Optical microscopy analysis was conducted to investigate the surface morphology of Krajood fiber-reinforced composites fabricated using different fiber sizes and varying fiber-to-binder ratios [13, 20]. Surface texture and uniformity are key indicators of fiber dispersion, binder penetration, and interfacial compatibility, which directly influence the composites' mechanical integrity and dimensional stability. Representative micrographs of each formulation are presented in Table 4.

The S-series composites exhibited generally smooth and uniform surface textures across all formulations. The S80I20 sample, containing the lowest fiber content (80%), showed slightly higher porosity and visible micro voids, possibly due to excess binder leading to fiber agglomeration and incomplete fiber wetting. In contrast, S85I15 displayed improved surface compactness with evenly distributed fibers and fewer observable voids, suggesting a more balanced ratio between fiber content and binder saturation. The surface of S90I10, with the highest fiber content (90%), appeared denser with closely packed fibers. However, minor fiber pull-outs were observed, likely resulting from insufficient binder to fully encapsulate and adhere to all fibers. These findings suggest that while increased fiber content enhances surface density, it may also compromise interfacial bonding if not adequately supported by binder volume [2, 6].

The L-series composites displayed more heterogeneous and rougher surfaces compared to the short fiber group. The increased fiber length led to pronounced surface protrusions and a higher incidence of fiber misalignment. In L80I20, fiber clustering and voids were particularly evident. L85I15 demonstrated improved morphology with better fiber distribution and reduced surface irregularities, indicating a more effective interaction between the longer fibers and the isocyanate resin. L90I10 presented a dense fiber network with reduced porosity; however, randomly oriented fibers introduced localized roughness and overlapping.

These features suggest that while long fiber enhances mechanical reinforcement, careful optimization of binder content and processing conditions is essential to minimize surface defects and ensure consistent fiber integration.

The M-series composites exhibited the most homogeneous and compact surface morphologies. The combination of short and long fibers facilitated efficient packing, with shorter fibers filling the voids between longer ones, thereby reducing overall porosity. M85I15 emerged as the most morphologically balanced formulation, featuring a continuous and tightly bound surface, well-integrated fibers, and minimal voids. This indicates a synergistic effect, where short fibers enhance binder dispersion and matrix filling, while long fibers contribute to structural reinforcement.

Optical microscopy images of Krajood composite surfaces with different fiber sizes and contents Table 4

Codes for composite surfaces of 10 mm (Short size)

S80I20 S85I15 S90I10

Codes for composite surfaces of 20 mm (Long size)

L80I20 L85I15 L90I10

Codes for composite surfaces of 10 and 20 mm (Mixed size)

M80I20 M85I15 M90I10

Although M90I10 maintained a compact surface, slight roughness due to localized long fiber protrusions was observed, underscoring the importance of sufficient binder at higher fiber loadings. M80I20, while slightly less uniform, still demonstrated superior fiber interlocking compared to single-size fiber composites. These observations confirm that mixed fiber lengths effectively enhance fiber-matrix interaction, crucial for optimizing surface quality and mechanical

performance.

Across all groups, the M-series composites exhibited the most favorable surface morphologies. The improved surface integrity observed in M85I15 and M90I10 highlights the effectiveness of hybrid fiber sizing in mitigating fiber misalignment and void formation commonly found in single-size composites. Furthermore, these surface morphology findings align with mechanical testing results, where mixed-size fiber composites showed enhanced tensile and flexural properties due to better fiber packing and interfacial bonding [14, 32]. In contrast, while the L-series composites offer mechanical advantages in terms of reinforcement, they also displayed greater surface irregularities that may impact long-term dimensional stability. The S-series, though smoother in appearance, may be limited in their load-bearing capacity under higher stress conditions.

4. Conclusions

This study comprehensively examined the mechanical, physical, acoustic, and morphological performance of Krajood fiber-reinforced wood-based composites bonded with isocyanate resin. By systematically varying fiber sizes and fiber-to-binder ratios, the research identified optimal configurations that significantly enhance both mechanical integrity and dimensional stability.

The findings demonstrated that tensile strength and hardness of the samples improved notably in composites incorporating M-series composites and balanced fiber-to-binder ratios, particularly at 85:15. This enhancement is attributed to the synergistic reinforcement enabled by effective fiber interlocking and improved matrix compatibility. In terms of physical behavior, water absorption and thickness swelling tests revealed that composites with higher binder content and short fibers were more resistant to moisture ingress, thereby promoting dimensional stability. The M-series composites further minimized water uptake by improving fiber packing density and limiting capillary pathways.

Acoustic performance testing showed that composites reinforced with L-series and M-series achieved superior sound absorption, especially in the mid-frequency range. This performance is linked to increased internal porosity and the extended paths for sound wave scattering created by the fiber network. Surface morphology observations using optical microscopy confirmed that composites containing mixed fiber sizes displayed the most compact, homogeneous, and defect-free surfaces. These surface characteristics are critical for applications requiring reliable interfacial bonding, high-quality surface finishes, and long-term durability.

The insights from this study have significant implications for sustainable and intelligent manufacturing in the bio-composite sector. Utilizing Krajood fibers a renewable agricultural by-product supports a shift toward eco-efficient, low-carbon production practices. Moreover, the improvements demonstrated through fiber hybridization and optimized binder content align with Industry 4.0 objectives for materials-by-design, offering the potential for predictive control of product quality using digital twins and AI-driven process modeling. With their favorable combination of mechanical performance, acoustic efficiency, and moisture resistance, these composites are particularly well-suited for applications

such as elderly-friendly furniture, interior acoustic panels, and bio-based construction materials. They represent a promising, sustainable alternative to conventional synthetic fiber-reinforced systems.

Acknowledgements

The authors gratefully acknowledge the financial support from the Thailand Science Research and Innovation (Research Grant Code: 66A171000025) and the Rajamangala University of Technology Srivijaya (RMUTSV), Thailand.

References

1. Alrubaie, M.A.A., Gardner, D.J., Lopez-Anido, R.A., 2020. Modeling the long-term deformation of a geodesic spherical frame structure made from wood plastic composite lumber. In: Applied Sciences, vol. 10(14), ID article 5017. DOI: 10.3390/app10145017.
2. Angelini, S., Barrio, A., Cerruti, P. et al., 2019. Lignosulfonates as fire retardants in wood flour-based particleboards. In: Journal of Polymer Science, vol. 4, ID article 6178163. DOI: 10.1155/2019/6178163.
3. ASTM D2240-91, 2021. Standard test method for rubber property – Durometer hardness. Advancing Standards Transforming Markets. PA, U.S.A.
4. ASTM D570-88, 2022. Standard test method for water absorption of plastics. Advancing Standards Transforming Markets. PA, U.S.A.
5. ASTM D638-91, 2022. Standard test method for tensile properties plastic. PA, U.S.A.
6. Barbos, J.D.V., Azevedo, J.B., Cardoso, P.S.M. et al., 2020. Development and characterization of WPCs produced with high amount of wood residue. In: Journal of Materials Research and Technology, vol. 9(5), pp. 9684-9690. DOI: 10.1016/j.jmrt.2020.06.073.
7. Bartlett, A.I., Hadden, R.M., Bisby, L.A., 2019. A review of factors affecting the burning behaviour of wood for application to tall timber construction. In: Fire Technology, vol. 55, pp. 1-49. DOI: 10.1007/s10694-018-0787-y.
8. Candelier, K., Atli, A., Alteyrac Eur, J., 2019. Termite and decay resistance of bioplast-spruce green wood-plastic composites. In: European Journal of Wood and Wood Products, vol. 77, pp. 157-169. DOI: 10.1007/s00107-018-1368-y.
9. Cherradi, Y., Rosca, I.C., Cerbu, C. et al., 2021. Acoustic properties for composite materials based on alfa and wood fibers. In: Applied Acoustics, vol. 174, ID article 107759. DOI: 10.1016/j.apacoust.2020.107759.
10. Elsheikh, A.H., Panchal, H., Shanmugan, S. et al., 2022. Recent progresses in wood-plastic composites: Pre-processing treatments, manufacturing techniques, recyclability and eco-friendly assessment. In: Cleaner Engineering and Technology, vol. 8, ID article 100450. DOI: 10.1016/j.clet.2022.100450.
11. Ferrari, F., Striani, R., Fico, D. et al., 2022. An overview on wood waste valorization as biopolymers and biocomposites: Definition, classification, production, properties and applications. In: Polymers, vol. 14(24), ID article 5519. DOI: 10.3390/polym14245519.

12. Hala, B., Kamal, G., Hamid, E. et al., 2016. Mechanical and thermal properties of hybrid composites: Oil-palm fiber/clay reinforced high density polyethylene. In: Mechanics of Materials, vol. 98, pp. 36-43. DOI: 10.1016/j.mechmat.2016.04.008.
13. Homkhiew, C., Cheewawuttipong, W., Srivabut, C. et al., 2025. Machinability of wood-plastic composites from the CNC milling process using the Box-Behnken design and response surface methodology for building applications. In: Journal of Thermoplastic Composite Materials, vol 38(1), pp. 161-187. DOI: 10.1177/0892705724124803.
14. Homkhiew, C., Srivabut, C., Boonchouytan, W. et al., 2024. Sandwich composites from recycled plastic reinforced with krajood (*Lepironia articulata*) fiber for building applications. In: Iranian Polymer Journal, vol. 33(6), ID article 839853. DOI: 10.1007/s13726-024-01292-y.
15. Homkhiew, C., Srivabut, C., Ratanawilai, T. et al., 2023. Characterization of polypropylene composites using sludge waste from the natural rubber latex industry as reinforcing filler. In: Journal of Material Cycles and Waste Management, vol. 25, pp. 1444-1456. DOI: 10.1007/s10163-023-01621-y.
16. ISO 10534-1, 1996. Acoustics – Determination of sound absorption coefficient and impedance in impedance tubes: Switzerland.
17. Kaymakci, A., Birinci, E., Ayrilmis, N., 2019. Surface characteristics of wood polypropylene nanocomposites reinforced with multi-walled carbon nanotubes. In: Composites Part B: Engineering, vol. 157, pp. 43-46. DOI: 10.1016/j.compositesb.2018.08.099.
18. Khamtree, S., Homkhiew, C., Srivabut, C. et al., 2025. Response surface optimization of hybrid composites reinforced crab shell flour and rubberwood sawdust for waterproof composite products in tropical countries. In: Journal of Material Cycles and Waste Management, vol. 27, pp. 1777-1800. DOI: 10.1007/s10163-025-02219-2.
19. Khamtree, S., Srivabut, C., Homkhiew, C. et al., 2023. The mechanical properties deterioration of rubberwood-latex sludge flour reinforced polypropylene composites after immersing in different water conditions. In: European Journal of Wood and Wood Products, vol. 81, pp. 1223-1237. DOI: 10.1007/s00107-023-01950-7.
20. Liu, H., Wang, J., Gong, C. et al., 2016. Morphology and mechanical properties of PVC/straw-fiber coated with liquid nitrile-butadiene rubber composites. In: Journal of Applied Polymer Science, vol. 133(43), ID article 44119. DOI: 10.1002/app.44119.
21. Ratanawilai, T., Taneerat, K., 2018. Alternative polymeric matrices for wood-plastic composites: Effects on mechanical properties and resistance to natural weathering. In: Construction and Building Materials, vol. 172, pp. 349-357. DOI: 10.1016/j.conbuildmat.2018.03.266.
22. Saha, A., Kumar, S., Zindani, D., 2021. Investigation of the effect of water absorption on thermomechanical and viscoelastic properties of flax-hemp-reinforced hybrid composite. In: Polymer Composites, vol. 42(9), pp. 4497-4516. DOI: 10.1002/pc.26164.

23. Sahu, P., Gupta, M.K., 2020. Water absorption behavior of cellulosic fibres polymer composites: A review on its effects and remedies. In: Journal of Industrial Textiles, vol. 51(5), pp. 7480-7512. DOI: 10.1177/1528083720974424.
24. Sair, S., Oushabi, A., Kammouni, A. et al., 2018. Mechanical and thermal conductivity properties of hemp fiber reinforced polyurethane composites. In: Case Studies in Construction Materials, vol. 8, pp. 203-212. DOI: 10.1016/j.cscm.2018.02.001.
25. Schmid, J., Just, A., Klippel, M. et al., 2015. The reduced cross-section method for evaluation of the fire resistance of timber members**:** discussion and determination of the zero-strength layer. In: Fire Technology, vol. 51, pp. 1285-1309. DOI: 10.1007/s10694-014-0421-6.
26. Srivabut, C., Homkhiew, C., Rawangwong, S. et al., 2022. Possibility of using municipal solid waste for manufacturing wood-plastic composites: Effects of natural weathering, wood waste types, and contents. In: Journal of Material Cycles and Waste Management, vol. 24, pp. 1407-1422. DOI: 10.1007/s10163-022-01443-4.
27. Srivabut, C., Ratanawilai, T., Hiziroglu, S., 2018. Effect of nanoclay, talcum, and calcium carbonate as filler on properties of composites manufactured from recycled polypropylene and rubberwood fiber. In: Construction and Building Materials, vol. 162, pp. 450-458. DOI: 10.1016/j.conbuildmat.2017.12.048.
28. Taban, E., Soltani, P., Berardi, U. et al., 2020. Measurement, modeling, and optimization of sound absorption performance of Kenaf fibers for building applications. In: Building and Environment, vol. 180, ID article 107087. DOI: 10.1016/j.buildenv.2020.107087.
29. Tan, W.H., Wahab, F., Mat, F. et al., 2024. Sound absorption coefficient measurement and analysis for multisection perforation microperforated panel. In: Journal of Mechanical Science and Technology, vol. 38, pp. 2797-2803. DOI: 10.1007/s12206-024-2210-6.
30. Wang, X., Yu, Z., McDonald, A.G., 2019. Effect of different reinforcing fillers on properties, interfacial compatibility and weatherability of wood-plastic composites. In: Journal of Bionic Engineering, vol. 16, pp. 337-353. DOI: 10.1007/s42235-019-0029-0.
31. Xiang, H.F., Wang, D., Liua, H.C. et al., 2013. Investigation on sound absorption properties of kapok fibers. In: Journal of Polymer Science, vol. 31, pp. 521-529. DOI: 10.1007/s10118-013-1241-8.
32. Zhou, Y., Wang, Y., Fan, M., 2019. Incorporation of tyre rubber into wood plastic composites to develop novel multifunctional composites: Interface and bonding mechanisms. In: Industrial Crops and Products, vol. 141, ID article 111788. DOI: 10.1016/j.indcrop.2019.111788.